Part II

Remediation of Selenium Contamination

Chapter 5

Reactivity and selectivity of zerovalent iron toward selenium oxyanions under aerobic conditions

Jinxiang Li, Yuankui Sun and Xiaohong Guan

5.1 AQUEOUS CHEMISTRY OF ZVI WITH SELENIUM

Zerovalent iron (ZVI, Fe^0) is readily available, inexpensive, reactive and environmentally friendly and thus has been widely used in sequestering various contaminants (Guan *et al.*, 2015; Johnson *et al.*, 1996; Li *et al.*, 2015a; Liang *et al.*, 2013, 2014a; Scherer *et al.*, 1998). It can undergo a series of corrosion reactions in the H_2O/O_2 system, including transformation of the released Fe^{2+}/Fe^{3+} (Figure 5.1), which are accompanied by the liberation of hydrogen and/or the reduction of oxygen (Guan *et al.*, 2015; Noubactep, 2008). Therefore, ZVI can act as not only a generator of adsorbing agents (i.e., iron (hydr)oxides) but also as an electron donor for the reduction of the selenium oxyanions, i.e. selenite (Se(IV)) and selenate (Se(VI)) (Fan *et al.*, 2019b; Noubactep, 2015).

Considering the redox-dependent solubility of selenium, as shown in Figure 5.1, the reduction of the soluble Se(IV) and Se(VI) to the insoluble Se(-II)/Se(0) by ZVI is a wise choice and of high environmental significance (Liang *et al.*, 2013; Shao *et al.*, 2018). Nevertheless, granular ZVI particles generally have low reactivity and utilization ratio toward Se(IV) and Se(VI) due to the resistance of the inherent or newly formed iron (hydr)oxides (Fan *et al.*, 2019a, b; Guo *et al.*, 2016; Li *et al.*, 2018, 2019, 2020a; Liang *et al.*, 2013, 2014a, b, 2015a, b; Qiao *et al.*, 2018; Tang *et al.*, 2014, 2016; Xu *et al.*, 2016; Zhang *et al.*, 2018, 2020),

doi: 10.2166/9781789061055_0173

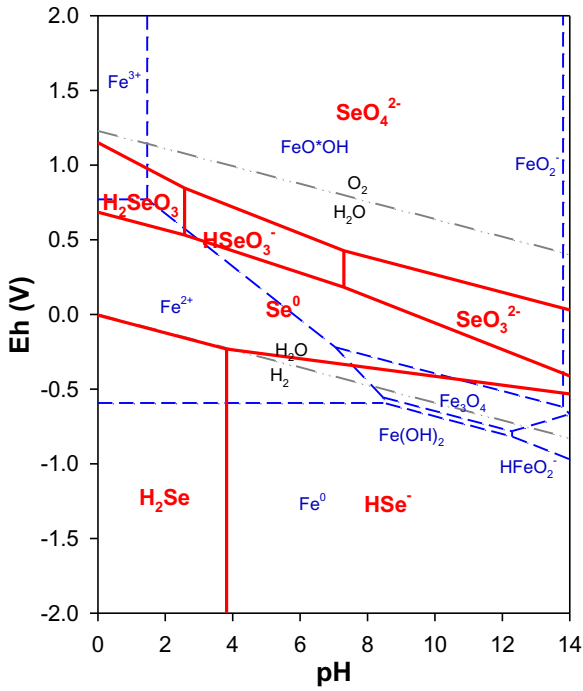

Figure 5.1 Eh-pH diagram for selenium in Fe^0/H_2O system at 298.15 K and 101.3 kPa (Qin *et al.*, 2016).

which can passivate ZVI and concurrently make the iron core (i.e., Fe^0) inaccessible. When applying ZVI to reduce Se(IV)/Se(VI) in the H_2O/O_2 system, the coexisting oxidizing compounds including H_2O, H^+, O_2, as well as other reducible species can compete with Se(IV)/Se(VI) for the electrons of ZVI, resulting in a low electron efficiency (EE) of ZVI. The parameter EE is defined as the proportion of electrons utilized by the reduction of the target contaminant to all available electrons provided by ZVI (Fan *et al.*, 2019a, b; Gu *et al.*, 2017; He *et al.*, 2020; Li *et al.*, 2017b, 2018, 2020a, b; Qiao *et al.*, 2018; Qin *et al.*, 2017).

In view of the limitations of ZVI-based technology, this chapter will systematically overview the performance of employing some promising strategies, such as imposing a weak magnetic field (WMF, see Section 5.2), dosing ferrous iron (see Section 5.3), and pre-treatment with sulfidation (see Section 5.4), to improve the reactivity and selectivity of ZVI toward Se(IV)/Se(VI). All the above-mentioned methods have gained great interest in recent years, while there are still some limitations in real practice. Thus, the corresponding suggestions for these three enhanced-ZVI technologies are further provided in Section 5.5.

5.2 WMF ENHANCES THE REACTIVITY AND SELECTIVITY OF ZVI TOWARD Se(IV) AND Se(VI)

5.2.1 Effect of WMF on the reactivity of ZVI toward Se(IV)/Se(VI)

The improvement of ZVI reactivity induced by a weak magnetic field (WMF) was first reported by Liang *et al.* (2014a). A WMF was found to significantly accelerate Se(IV) removal and extend the working pH range of ZVI from 4.0–6.0 (without WMF) to 4.0–7.2 (with WMF). Since the WMF can be applied by two pieces of permanent magnet, the WMF-assisted ZVI technology is environmentally friendly and thus promising for real applications such as groundwater/wastewater remediation/treatment (Guan *et al.*, 2015; Liang *et al.*, 2014b; Reinsch *et al.*, 2010; Sarathy *et al.*, 2008; Wang *et al.*, 2010).

The positive effect of a WMF on Se(IV)/Se(VI) removal by ZVI under various reaction conditions has been extensively reported (Li *et al.*, 2020a; Liang *et al.*, 2014b; Xu *et al.*, 2016; Zhang *et al.*, 2018), as shown in Figure 5.2. Besides pristine ZVI (Pri-ZVI), the performance of aged ZVI (AZVI) with WMF has also been explored (Guan *et al.*, 2015; Liang *et al.*, 2014b; Reinsch *et al.*, 2010; Sarathy *et al.*, 2008; Wang *et al.*, 2010). A WMF could significantly enhance the reactivity of all AZVI samples prepared under different background matrices and aging durations. Moreover, the WMF enhancing effect could enable a high reactivity of ZVI collected from different origins toward both Se(IV) and Se(VI) removal to various extents.

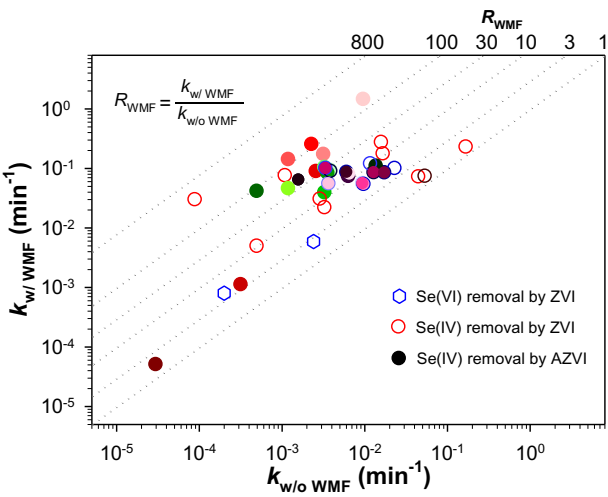

Figure 5.2 Rate constants for sequestration of Se(IV) and Se(VI) with and without WMF by ZVI and AZVI (Zhang *et al.*, 2018).

In order to better illustrate the enhancing effect of WMF on the reactivity of the ZVI/AZVI, the wide spectrum of rate constants (min^{-1}) of the pseudo-first-order kinetics for sequestration of Se(IV) and Se(VI) were compared by the ratio R_{WMF} (formulated in Figure 5.2), where $k_{w/\,WMF}$ and $k_{w/o\,WMF}$ are the corresponding observed rate constants with and without WMF, respectively. Figure 5.2 shows that the R_{WMF} mainly falls in the range of 3.0–100.0, with only a few cases outside of this range. As compared to the R_{WMF} values (i.e., 2.5–4.0) for Se(VI) removal, a WMF induced greater enhancement in Se(IV) removal by ZVI with R_{WMF} values ranging from 1.3 to 330.4. Furthermore, it should be noted that the enhancing effects of a WMF on AZVI samples were more outstanding than those of Pri-ZVI based on a wide-spectrum analysis (Li *et al.*, 2015a, b, 2016, 2017a; Sun *et al.*, 2014, 2017; Zhang *et al.*, 2018), which may be associated with the promotion of mass transfer and the enrichment of reactants by the synergistic effects of a WMF and iron (hydr)oxides.

5.2.2 Effect of WMF on the selectivity of ZVI toward Se(IV)/Se(VI)

After elucidating the improved reactivity of ZVI by the WMF, the undesired reactions of ZVI with the non-target compounds (e.g., O_2 and H_2O/H^+) may be concurrently inhibited (Gu *et al.*, 2017; He *et al.*, 2020; Li *et al.*, 2017b, 2018, 2020b; Qiao *et al.*, 2018; Zhang *et al.*, 2020). There may be a trade-off between the reactivity and electron selectivity of ZVI in the presence of WMF (Qiao *et al.*, 2018). As such, this section mainly focused on the effect of a WMF on the electron utilization (EU) and electrical efficiency (EE) of ZVI toward Se(IV) and Se(VI). Based on the detailed studies of selenium removal by ZVI/WMF via diverse spectral protocols, it was revealed that WMF could not only accelerate the corrosion of ZVI during Se decontamination, but also facilitate the transformation of Se(IV)/Se(VI) to Se(0) (Li *et al.*, 2020a; Liang *et al.*, 2014a, b; Xu *et al.*, 2016). However, it was found that the corresponding EU values were almost identical when the reactions between Se(IV)/Se(VI) and ZVI reach equilibrium, as shown in Figure 5.3a.

Since applying a WMF can tune the mechanism of Se(IV) removal by ZVI from adsorption followed by reduction to direct reduction (Liang *et al.*, 2014a, b), it suggests that a WMF can improve the electron transport in the ZVI, thus enhancing the EE of ZVI for selenium reduction. As plotted in Figure 5.3b, the EE of ZVI with WMF for reduction of Se(IV)/Se(VI) was 3.7- to 14.1-fold greater than that without WMF, regardless of the 'single' or 'multiple' dosing mode (Li *et al.*, 2020a). In addition, the EE of ZVI/WMF toward Se(IV) was higher than that toward Se(VI), which was likely due to the different involvement of the redox ability and affinity between Se(IV) and Se(VI) (Li *et al.*, 2020a).

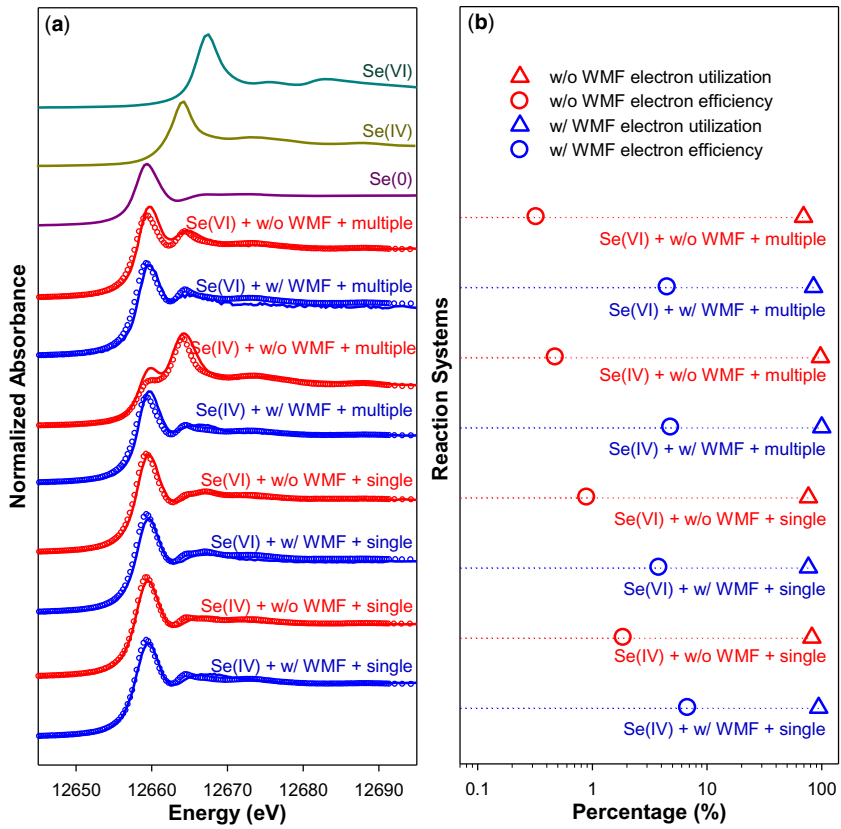

Figure 5.3 Se *K*-edge XANES spectra (a) of the Se-treated ZVI samples at sequestration equilibrium, along with the corresponding active parameters (b) of ZVI. The circles and the thick lines represent the linear combination fits and the experimental data, respectively (Li *et al.*, 2020a).

5.2.3 Contributions of WMF to the improved reactivity and selectivity of ZVI toward Se(IV)/Se(VI)

As for the genesis of enhanced reactivity and selectivity, Liang *et al.* (2014a) and Sun *et al.* (2014) showed that a WMF could accelerate the corrosion of ZVI and the transformation of amorphous iron (hydr)oxides to lepidocrocite, which favored the contaminant sequestration. Besides, under aerobic conditions, Li *et al.* (2016) further confirmed that the enhancing effect of WMF was mainly ascribed to the magnetic field gradient force ($F_{\Delta B}$), which can drive the movement of paramagnetic Fe^{2+} toward the site with higher induced magnetic field. Following this study, Sun *et al.* (2017) further demonstrated the coupled effect of coexisting anions and WMF on the enhanced reactivity of ZVI, which

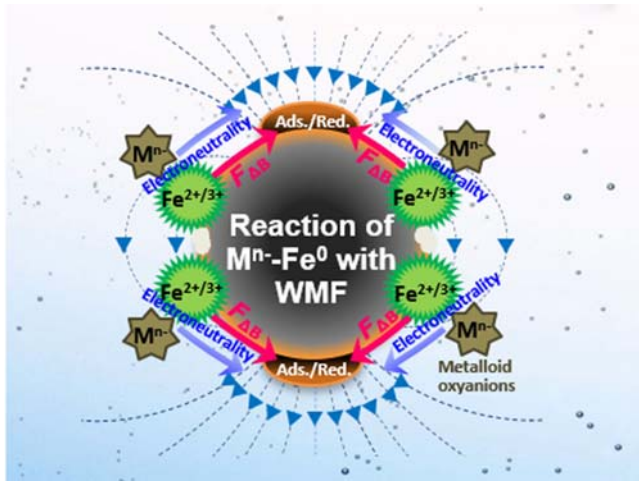

Figure 5.4 Proposed schematic illustration of the reactions of ZVI with Se(IV)/Se(VI) in the presence of a WMF (Li *et al.*, 2020a).

was associated with the simultaneous movement of anions and paramagnetic Fe^{2+} to keep local electroneutrality in the solution. Likewise, the movement of an anionic target should be also reflected by the transportation of paramagnetic Fe^{2+} in the ZVI/WMF system. As such, the $F_{\Delta B}$ induced by a WMF can selectively drive the metalloid oxyanions, including Se(IV) and Se(VI), toward the *in situ* formed iron (hydr)oxides, thereby leading to an enhanced reactivity and specific removal capacity (SRC) of ZVI toward the metalloid oxyanions (Li *et al.*, 2020a).

Considering that enrichment is the first step of electron transfer from the Fe^0 core to the target, the efficient incorporation of a contaminant into the iron corrosion products in the presence of a WMF is beneficial to the EE of ZVI for the reduction of Se(IV) and Se(VI). In general, it could be reasonably inferred that the improved reactivity and selectivity of ZVI toward Se(IV) and Se(VI) induced by a WMF is mainly ascribed to the $F_{\Delta B}$-derived movement of paramagnetic Fe^{2+} with Se(IV)/Se(VI) for the local electroneutrality at the ZVI reaction interface, as depicted in Figure 5.4. In summary, WMF is a promising and environmentally friendly method to enhance the reactivity and selectivity of ZVI toward the Se(IV) and Se(VI) under aerobic conditions.

5.3 FERROUS ION ENHANCES THE REACTIVITY AND SELECTIVITY OF ZVI TOWARD Se(VI)

5.3.1 Influence of Fe(II) on the reactivity of ZVI towards Se(VI)

Recently, the research on contaminant removal by ZVI has greatly increased the dimensions of complexity in this area (Shao *et al.*, 2018). Since Fe(II) and

aerobic conditions are two of the most broadly relevant parameters, this section introduces the dynamic interactions between Fe(II) and O_2 on the reactivity and selectivity of ZVI towards Se(IV). As shown in Figure 5.5, the removal capacity and rate of Se(VI) by ZVI increased with an increase in the Fe(II) concentration from 0 to 1.0 mM and the enhancement was greater at higher oxygen concentration (He *et al.*, 2020; Li *et al.*, 2020a; Qiao *et al.*, 2018; Qin *et al.*, 2017). It was found that oxygen is essential for the sequestration of Se(VI) by ZVI. On the one hand, specifically, the SRC of ZVI towards Se(VI) increased progressively from 17.7–24.7 to 49.2–49.9 mg/g with an increase in the initial concentration of Fe(II) from 0 to 1.0 mM under aerobic conditions (Figure 5.5a). On the other hand, oxygen and Fe(II) showed a synergistic effect on the removal rate of Se(VI) by ZVI, which implies that the presence of Fe(II) had a greater accelerating effect on Se(VI) removal by ZVI at high oxygen concentrations (Qin *et al.*, 2017), and vice versa.

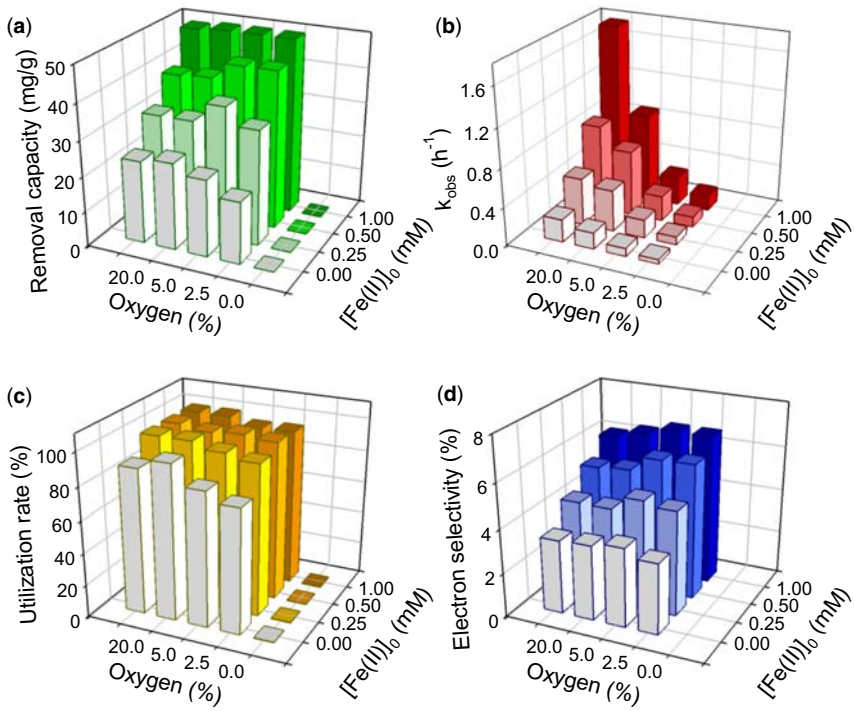

Figure 5.5 Influence of oxygen volume fraction in the purging gas and Fe(II) concentration on (a) capacity and (b) pseudo-first order rate constants (k_{obs}) of Se (VI) removal by ZVI as well as on utilization rate (c), and electron selectivity (d) of ZVI (Qin *et al.*, 2017).

5.3.2 Influence of Fe(II) on the selectivity of ZVI towards Se(VI)

Figure 5.5c shows Fe(II) dosing enhances the utilization ratio (UR) of ZVI to a greater extent at a lower oxygen fraction in the sparging gas (i.e., 2.5–5.0%) than at a higher oxygen fraction (i.e., 20.0–50.0%). Correspondingly, the UR values of ZVI for Se(VI) sequestration at oxygen fractions of 2.5, 5.0, 20, and 50% were increased by 19.4, 12.7, 5.0, and 11.0%, respectively, when the initial Fe(II) concentration increased from 0 to 1.0 mM. Furthermore, there are two obvious trends in the electron selectivity or EE of ZVI toward Se(VI) under different conditions. First, the EE of ZVI for Se(VI) reduction under aerobic conditions increased progressively from 3.2–3.6% to 6.2–6.8% as the initial Fe(II) concentration increased from 0 to 1.0 mM. Second, regardless of the initial Fe(II) concentration, the EE of ZVI improved slightly by increasing the oxygen fraction in the sparging gas from 2.5% to 5.0%. However, a further increase in the oxygen fraction resulted in only a slight drop in the EE of ZVI.

5.3.3 Role of Fe(II) in improving the reactivity and selectivity of ZVI for Se(VI) reduction

The sequestration of Se(VI) by ZVI is a heterogeneous redox reaction at the ZVI-H_2O interface, thus the mass transfer of Se(VI) toward the ZVI surface is a prerequisite of Se(VI) reduction by the electrons from the Fe^0 core. Characterization results suggested that with the increase of the initial Fe(II) concentration, the fractions of Fe^0 and γ-Fe_2O_3 in the Se(VI)-treated ZVI under aerobic conditions dropped, while that of lepidocrocite (γ-FeOOH) and magnetite (Fe_3O_4) increased (Qin *et al.*, 2017), which enhanced Se(VI) adsorption and the subsequent electron transfer between the underlying Fe^0 and the surface-decorated Se(VI). As shown in Figure 5.6, the Fe(II)-induced improvement in the rate constants of Se(VI) sequestration by Fe^0 and the electron selectivity of Fe^0 towards Se(VI) under aerobic conditions were attributed to the weak acidity arising from the Fe(II) addition (Huang and Zhang, 2005; Liu *et al.*, 2013) and the facilitated Se VI) enrichment by the γ-FeOOH, along with the favored electron conductivity by Fe_3O_4 generated on the surface of the ZVI particle.

5.4 SULFIDATION TREATMENT ENHANCES THE REACTIVITY AND SELECTIVITY OF ZVI TOWARD Se(VI)

Sulfidation of ZVI has gained increased attention due to its positive role in enhancing both the reactivity and selectivity of ZVI under anaerobic conditions (Fan *et al.*, 2016, 2017; He *et al.*, 2018; Li *et al.*, 2017b; Qin *et al.*, 2019; Rajajayavel and Ghoshal, 2015). Hydrogen production during reaction of ZVI

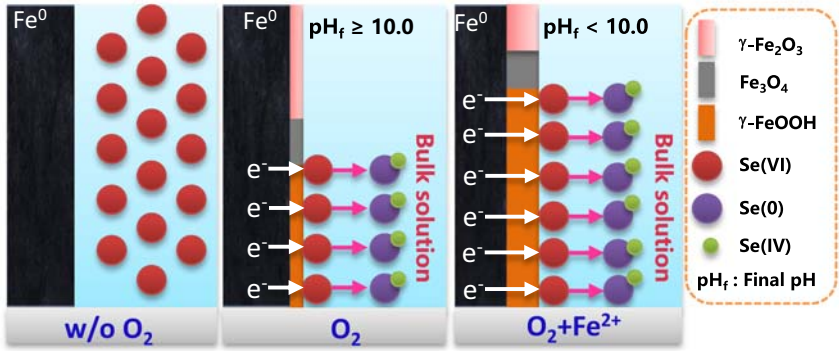

Figure 5.6 Proposed mechanistic model for the influence of oxygen and Fe(II) on Se(VI) removal by ZVI (w/o O_2: without O_2) (Qin *et al.*, 2017).

with water is suppressed by sulfidation under anaerobic conditions, thus leading to an increase in the selectivity of ZVI toward contaminant reduction. Considering the potential application of sulfidated ZVI (S-ZVI) in wastewater treatment, where dissolved oxygen is commonly present and is a much stronger electron acceptor than water, the influence of sulfidation on the reactivity and selectivity of ZVI under aerobic conditions needs to be understood. Hence, this section discusses the impacts of sulfidation on the reactivity and selectivity of ZVI toward Se (VI) reduction.

5.4.1 Influence of sulfidation on the reactivity of ZVI toward Se(VI)

With regard to the reactivity of S-ZVI, Qiao *et al.* (2018) systematically compared the Se(VI) reduction performance of unamended ZVI and sulfidated ZVI in the presence of different coexisting ions including Cl^-, SO_4^{2-}, PO_4^{3-}, Ca^{2+}, and Mg^{2+} under aerobic conditions. Compared with the ball-milled ZVI without elemental S (ZVI^{bm}), S-ZVI synthesized by ball-milling with elemental sulfur ($S\text{-}ZVI^{bm}$) enhanced the reactivity of ZVI toward Se(VI), whereas the positive effect was not very pronounced in the presence of some specific background electrolytes. For example, at reaction equilibrium, sulfidation increased the Se (VI) removal capacity of ZVI from ~15.6 to 30.4 mg/g in the presence of 1 mM Cl^-, whereas there was no noticeable influence when further increasing the Cl^- concentration to 10 and 20 mM (Qiao *et al.*, 2018). Taking the 10 mM NaCl case as a benchmark, it was further found that the presence of SO_4^{2-} or PO_4^{3-} inhibits the Se(VI) removal capacity of $S\text{-}ZVI^{bm}$ (still higher than that of ZVI^{bm}), which became more remarkable with further increasing of the anion concentration (Qiao *et al.*, 2018). On the contrary, the hardness ions could increase the removal

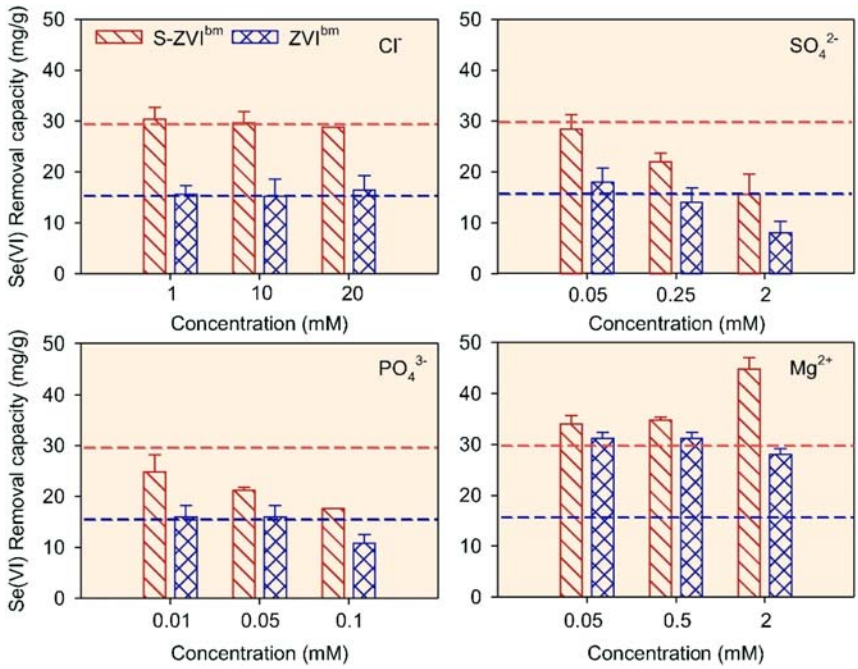

Figure 5.7 Comparison of the removal capacity of ZVI^{bm} and S-ZVI^{bm} toward Se(VI) in the presence of different coexisting ions. Reaction conditions: $[ZVI]_0 = 0.5$ g/L, $[Se(VI)]_0 = 40$ mg/L, $pH_{ini} = 5.0$, $T = 25$ °C, reaction time = 24 h. The horizontal lines reflect the Se(VI) removal capacity of ZVI^{bm} (blue) and S-ZVI^{bm} (red) obtained in 10 mM NaCl benchmark solutions (Qiao *et al.*, 2018).

capacity from 29.6 mg/g to as high as 44.8 mg/g with 2.0 mM Mg^{2+}, as depicted in Figure 5.7.

5.4.2 Influence of sulfidation on the selectivity of ZVI toward Se(VI)

With respect to the selectivity of S-ZVI toward Se(VI), the different coexisting ions could either negligibly, positively or negatively impact the EE of ZVI toward Se (VI), depending on their types and concentrations (Qiao *et al.*, 2018). On the one hand, NaCl did not greatly affect the EE of S-ZVI^{bm}, whereas the presence of SO_4^{2-} and PO_4^{3-} suppressed it, especially at relatively high concentrations (Figure 5.8). On the other hand, Mg^{2+} improved the selectivity of ZVI and a maximum EE value of 8.8% was obtained with the introduction of 2 mM Mg^{2+}. In general, this study sheds some light on evaluating the broader applicability of sulfidation and designing optimal operating conditions for the desirable ZVI performance (Qiao *et al.*, 2018).

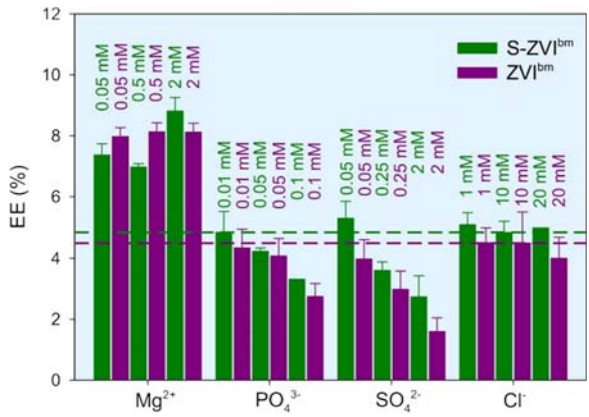

Figure 5.8 Effect of coexisting ions on the EE of ZVI^{bm} and S-ZVI^{bm} toward Se(VI) (Qiao *et al.*, 2018).

5.4.3 Coupled effects of sulfidation and ferrous dosing on Se(VI) removal by ZVI

In light of the improvements of ZVI selectivity toward Se(VI) (Li *et al.*, 2020a; Qin *et al.*, 2017), it is likely that the EE of the aerobic ZVI system can be enhanced via regulating its corrosion behavior. Sulfidation may impact the selectivity of ZVI since it can influence the Fe^0 corrosion behavior. All of Fe^0 in S-ZVI^{bm} was exhausted within 24 h with lepidocrocite and magnetite being the primary corrosion products (Qiao *et al.*, 2018). This suggested that the coexisting ions may influence the EE by affecting Se(VI) adsorption and the subsequent electron transfer from the Fe^0 core to Se(VI) at the water-particle interface. Given these facts, Fan *et al.* (2019b) further confirmed that sulfidation coupled with Fe (II) dosing could synergistically improve the reactivity and selectivity of ZVI toward Se(VI) under aerobic conditions (Figure 5.9). The promoting effect on Se (VI) sequestration by S-ZVI/Fe^{2+} is mainly associated with the following aspects: (1) Fe^{2+} could maintain a relatively low pH level during Se(VI) removal by S-ZVI; (2) S-ZVI/Fe^{2+} could retard the consumption of Fe^0 by the non-target O_2/H^+, thus facilitating the EE of S-ZVI; and (3) Fe(II) dosing could enable the electron transfer by forming semiconductive Fe_3O_4.

5.5 OUTLOOK

The superposition of WMF, Fe(II) dosing, and sulfidation pre-treatment can greatly improve the reactivity and selectivity of ZVI toward Se(IV)/Se(VI) under aerobic conditions, but to diverse extents. Among these three enhanced-ZVI technologies, ZVI/Fe^{2+} attained the largest amount of Se(VI) sequestration, while S-ZVI had the highest k_{obs} for removing Se(VI) (Figure 5.10). As for the removal

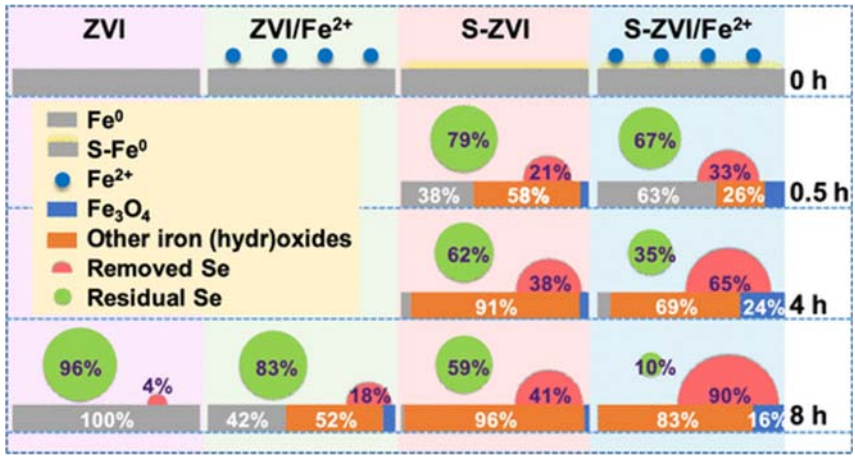

Figure 5.9 Coupled effects of sulfidation and ferrous dosing on Se(VI) removal by ZVI (Fan *et al.*, 2019b).

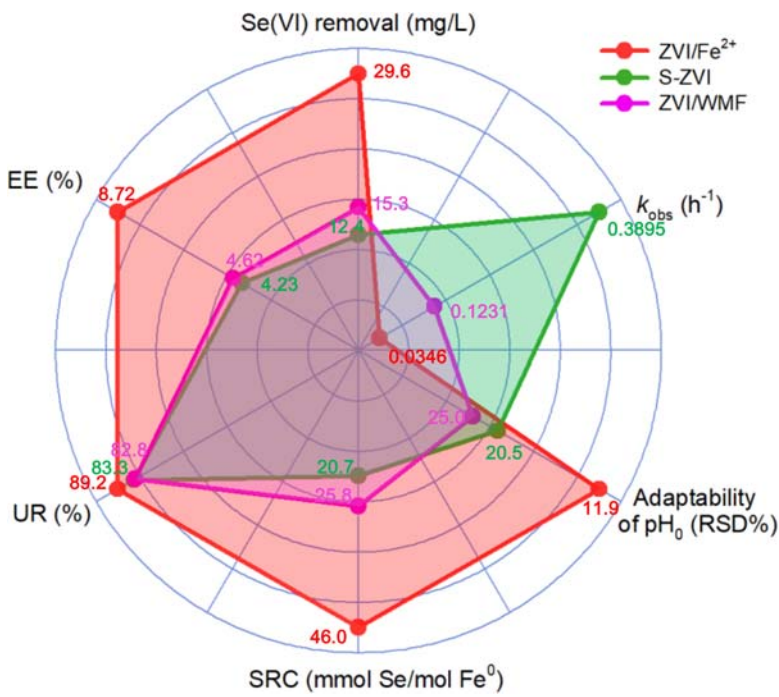

Figure 5.10 Comprehensive comparison of the performance of Se(VI) sequestration by ZVI/WMF, ZVI/Fe^{2+} and S-ZVI systems (Fan *et al.*, 2019a).

mechanism of Se(VI), these three enhancing techniques did not change the reaction mechanism of Se(VI) with ZVI, but only affected the rates and amounts of Se(VI) removal by ZVI. In theory, these enhancing techniques accelerate the corrosion of ZVI and tune the corresponding products transformation for better mass transfer of Se(IV)/Se(VI) (Fan *et al.*, 2019a, b; Li *et al.*, 2020a; Qiao *et al.*, 2018; Qin *et al.*, 2017), confirming that the corrosion of ZVI is a necessity and induces the removal of contaminants by ZVI. Considering the amount of removed Se(VI), the ZVI/Fe^{2+} system seems to be superior to the two other enhanced-ZVI technologies in terms of the utilization efficiency of ZVI at the end of reaction, and the adaptability over a wide pH range, as well as the chemical cost (Fan *et al.*, 2019a). Therefore, future research should focus on illustrating the performance of the ZVI/Fe^{2+} system toward Se(VI) on a pilot-scale (Fan *et al.*, 2019a). Moreover, the feasibility of employing Fe^{2+} to enhance the performance of ZVI should be examined with ZVI of different origins, different target contaminants, and in the presence of different background matrices (Fan *et al.*, 2019a), as well as coupled with WMF or sulfidation (Fan *et al.*, 2019b).

REFERENCES

Fan D., O'Brien Johnson G. S., Tratnyek P. G. and Johnson R. L. (2016). Sulfidation of nano zerovalent iron (nZVI) for improved selectivity during in-situ chemical reduction (ISCR). *Environmental Science Technology*, **50**(17), 9558–9565.

Fan D., Lan Y., Tratnyek P. G., Johnson R. L., Filip J., O'Carroll D. M., Nunez Garcia A. and Agrawal A. (2017). Sulfidation of iron-based materials: A review of processes and implications for water treatment and remediation. *Environmental Science Technology*, **51**, 13070–13085.

Fan P., Li L., Sun Y., Qiao J., Xu C. and Guan X. (2019a). Selenate removal by Fe^0 coupled with ferrous iron, hydrogen peroxide, sulfidation, and weak magnetic field: a comparative study. *Water Research*, **159**, 375–384.

Fan P., Sun Y., Zhou B. and Guan X. (2019b). Coupled effect of sulfidation and ferrous dosing on selenate removal by zerovalent iron under aerobic conditions. *Environmental Science Technology*, **53**(24), 14577–14585.

Gu Y., Wang B., He F., Bradley M. J. and Tratnyek P. G. (2017). Mechanochemically sulfidated microscale zero valent iron: pathways, kinetics, mechanism, and efficiency of trichloroethylene dechlorination. *Environmental Science Technology*, **51**(21), 12653–12662.

Guan X. H., Sun Y. K., Qin H. J., Li J. X., Lo I. M., He D. and Dong H. R. (2015). The limitations of applying zero-valent iron technology in contaminants sequestration and the corresponding countermeasures: the development in zero-valent iron technology in the last two decades (1994–2014). *Water Research*, **75**, 224–248.

Guo X. J., Yang Z., Dong H. Y., Guan X. H., Ren Q. D., Lv X. F. and Jin X. (2016). Simple combination of oxidants with zero-valent-iron (ZVI) achieved very rapid and highly efficient removal of heavy metals from water. *Water Research*, **88**, 671–680.

He F., Li Z., Shi S., Xu W., Sheng H., Gu Y., Jiang Y. and Xi B. (2018). Dechlorination of excess trichloroethene by bimetallic and sulfidated nanoscale zero-valent iron. *Environmental Science Technology*, **52**(15), 8627–8637.

He F., Gong L., Fan D., Tratnyek P. G. and Lowry G. V. (2020). Quantifying the efficiency and selectivity of organohalide dechlorination by zerovalent iron. *Environmental Science Processes & Impacts*, **22**, 528–542.

Huang Y. H. and Zhang T. C. (2005). Effects of dissolved oxygen on formation of corrosion products and concomitant oxygen and nitrate reduction in zero-valent iron systems with or without aqueous Fe^{2+}. *Water Research*, **39**(9), 1751–1760.

Johnson T. L., Scherer M. M. and Tratnyek P. G. (1996). Kinetics of halogenated organic compound degradation by iron metal. *Environmental Science Technology*, **30**(8), 2634–2640.

Li J., Qin H. and Guan X. (2015a). Premagnetization for enhancing the reactivity of multiple zerovalent iron samples toward various contaminants. *Environmental Science Technology*, **49**(24), 14401–14408.

Li J., Shi Z., Ma B., Zhang P., Jiang X., Xiao Z. and Guan X. (2015b). Improving the reactivity of zerovalent iron by taking advantage of its magnetic memory: implications for arsenite removal. *Environmental Science Technology*, **49**(17), 10581–10588.

Li J., Qin H., Zhang W. X., Shi Z., Zhao D. and Guan X. (2016). Enhanced Cr(VI) removal by zero-valent iron coupled with weak magnetic field: role of magnetic gradient force. *Separation and Purification Technology*, **176**, 40–47.

Li J., Qin H., Zhang X. and Guan X. (2017a). Improving the reactivity of zerovalent iron toward various contaminants by weak magnetic field: Performances and Mechanisms. *Acta Chimica Sinica*, **75**(6), 544.

Li J., Zhang X., Sun Y., Liang L., Pan B. C., Zhang W. and Guan X. (2017b). Advances in sulfidation of zerovalent iron for water decontamination. *Environmental Science Technology*, **248**(23), 173–182.

Li J., Zhang X., Liu M., Pan B. C., Zhang W., Shi Z. and Guan X. (2018). Enhanced reactivity and electron selectivity of sulfidated zerovalent iron toward chromate under aerobic conditions. *Environmental Science Technology*, **52**(5), 2988–2997.

Li J., Dou X. M., Qin H., Sun Y. K., Yin D. Q. and Guan X. (2019). Characterization methods of zerovalent iron for water treatment and remediation. *Water Research*, **148**, 70–85.

Li J., Sun Y., Zhang X. and Guan X. (2020a). Weak magnetic field enables high selectivity of zerovalent iron toward metalloid oxyanions under aerobic conditions. *Journal of Hazardous Materials*, **400**, 123330.

Li M., Mu Y., Shang H., Mao C., Cao S., Ai Z. and Zhang L. (2020b). Phosphate modification enables high efficiency and electron selectivity of nZVI toward Cr(VI) removal. *Applied Catalysis B-Environmental*, **263**, 118364.

Liang L., Yang W., Guan X., Li J., Xu Z., Wu J., Huang Y. and Zhang X. (2013). Kinetics and mechanisms of pH-dependent selenite removal by zero valent iron. *Water Research*, **47**(15), 5846–5855.

Liang L., Sun W., Guan X., Huang Y., Choi W., Bao H., Li L. and Jiang Z. (2014a). Weak magnetic field significantly enhances selenite removal kinetics by zero valent iron. *Water Research*, **49**, 371–380.

Liang L. P., Guan X. H., Shi Z., Li J. L., Wu Y. N. and Tratnyek P. G. (2014b). Coupled effects of aging and weak magnetic fields on sequestration of selenite by zero-valent iron. *Environmental Science Technology*, **48**(11), 6326–6334.

Liang L., Guan X., Huang Y., Ma J., Sun X., Qiao J. and Zhou G. (2015a). Efficient selenate removal by zero-valent iron in the presence of weak magnetic field. *Separation and Purification Technology*, **156**, 1064–1072.

Liang L., Jiang X., Yang W., Huang Y., Guan X. and Li L. (2015b). Kinetics of selenite reduction by zero-valent iron. *Desalination and Water Treatment*, **53**(9), 2540–2548.

Liu T., Li X. and Waite T. D. (2013). Depassivation of aged Fe^0 by ferrous ions: implications to contaminant degradation. *Environmental Science Technology*, **47**(23), 13712–13720.

Noubactep C. (2008). A critical review on the process of contaminant removal in Fe^0-H_2O systems. *Environmental Technology*, **29**(8), 909–920.

Noubactep C. (2015). Metallic iron for environmental remediation: a review of reviews. *Water Research*, **85**, 114–123.

Qiao J., Song Y., Sun Y. and Guan X. (2018). Effect of solution chemistry on the reactivity and electron selectivity of zerovalent iron toward Se(VI) removal. *Chemical Engineering Journal*, **353**, 246–253.

Qin H. J., Li J. X., Bao Q. Q., Li L. N. and Guan X. H. (2016). Role of dissolved oxygen in metal(loid) removal by zerovalent iron at different pH: its dependence on the removal mechanisms. *RSC Advances*, **6**, 50144–50152.

Qin H. J., Li J. X., Yang H. Y., Pan B. C., Zhang W. M. and Guan X. H. (2017). Coupled effect of ferrous ion and oxygen on the electron selectivity of zerovalent iron for selenate sequestration. *Environmental Science Technology*, **51**(9), 5090–5097.

Qin H., Guan X. and Tratnyek P. G. (2019). Effects of sulfidation and nitrate on the reduction of N-Nitrosodimethylamine by zerovalent iron. *Environmental Science Technology*, **53**(16), 9744–9754.

Rajajayavel S. R. and Ghoshal S. (2015). Enhanced reductive dechlorination of trichloroethylene by sulfidated nanoscale zerovalent iron. *Water Research*, **78**, 144–153.

Reinsch B. C., Forsberg B., Penn R. L., Kim C. S. and Lowry G. V. (2010). Chemical transformations during aging of zerovalent iron nanoparticles in the presence of common groundwater dissolved constituents. *Environmental Science Technology*, **44**(9), 3455–3461.

Sarathy V., Tratnyek P. G., Nurmi J. T., Baer D. R., Amonette J. E., Chun C. L., Penn R. L. and Reardon E. J. (2008). Aging of iron nanoparticles in aqueous solution: effects on structure and reactivity. *Journal of Physical Chemistry C*, **112**(7), 2286–2293.

Scherer M. M., Balko B. A., Gallagher D. A. and Tratnyek P. G. (1998). Correlation analysis of rate constants for dechlorination by zero-valent iron. *Environmental Science Technology*, **32**(19), 3026–3033.

Shao Q., Xu C., Wang Y., Huang S., Zhang B., Huang L., Fan D. and Tratnyek P. G. (2018). Dynamic interactions between sulfidated zerovalent iron and dissolved oxygen: mechanistic insights for enhanced chromate removal. *Water Research*, **135**, 322–330.

Sun Y. K., Guan X. H., Wang J. M., Meng X. G., Xu C. H. and Zhou G. M. (2014). Effect of weak magnetic field on arsenate and arsenite removal from water by zerovalent iron: an XAFS investigation. *Environmental Science Technology*, **48**(12), 6850–6858.

Sun Y., Hu Y., Huang T., Li J., Qin H. and Guan X. (2017). Combined effect of weak magnetic field and anions on arsenite sequestration by zero-valent iron: kinetics and

mechanisms. *Environmental Science Technology*, **51**(7), 3742–3750. doi:10.1021/acs.est.6b06117

Tang C. L., Huang Y. H., Zeng H. and Zhang Z. Q. (2014). Reductive removal of selenate by zero-valent iron: the roles of aqueous Fe^{2+} and corrosion products, and selenate removal mechanisms. *Water Research*, **67**, 166–174.

Tang C. L., Huang Y. P., Zhang Z. Q., Chen J. J., Zeng H. and Huang Y. H. (2016). Rapid removal of selenate in a zero-valent iron/Fe_3O_4/Fe^{2+} synergetic system. *Applied Catalysis B-Environmental*, **184**, 320–327.

Wang Q., Lee S. and Choi H. (2010). Aging study on the structure of Fe 0 nanoparticles: stabilization, characterization, and reactivity. *Journal of Physical Chemistry, C* **114**, 2027–2033.

Xu H., Sun Y., Li J., Li F. and Guan X. (2016). Aging of zerovalent iron in synthetic groundwater: X-ray photoelectron spectroscopy depth profiling characterization and depassivation with uniform magnetic field. *Environmental Science Technology*, **50**(15), 8214–8222.

Zhang X., Li J., Sun Y., Li L., Pan B., Zhang W. and Guan X. (2018). Aging of zerovalent iron in various coexisting solutes: characteristics, reactivity toward selenite and rejuvenation by weak magnetic field. *Separation and Purification Technology*, **191**, 94–100.

Zhang J., Cheng Z., Yang X., Luo J., Li H., Chen H., Zhang Q. and Li J. (2020). Mediating the reactivity and selectivity of nanoscale zerovalent iron toward nitrobenzene under porous carbon confinement. *Chemical Engineering Journal*, **393**, 124779.